Bhoo-Kampan Vol. 1, pp.1-20, December 2014

http://bhookampan.co.in/index.php
Journal of Indian Society of Earthquake Science
Publisher ISES *ISSN:2320-6217*

Finite Element Analysis of Buried Continuous Pipeline Subjected to Large Ground Motion

Vasudeo Chaudhari[1], Venkata Dilip Kumar P[2], Ramancharla Pradeep Kumar[2]*

[1]Civil Engineering Department, Indus University, Ahmedabad, Gujarat 382721, India
[2]Earthquake Engineering Research Centre, International Institute of Information Technology, Hyderabad, India.

Received: 28/02/2013; Accepted: 19/04/2014

Abstract

Pipeline generally extends over long distances traversing through wide variety of different soils, geological conditions and regions with different seismicity and ground motions. Vulnerability of the pipeline due to seismic hazards can be divided into three categories i.e. hazard due to ground vibration, hazard due to faulting and hazard due to permanent ground deformation (PGD). Though there are no severe damages observed due to ground vibration in the modern buried pipelines, damage may be triggered due to secondary effect of land-sliding and ground motion due to liquefaction. Main stream researches in the past, especially analytical models are limited to strike slip fault motions with tension in pipe case only. Even though incorporating the large geometric changes in analytical study is a tricky task, pipeline subjected to the large ground motion itself is a phenomenon of large geometric changes. Especially when pipeline is subjected to compression, where in addition to material deformation, it also undergoes general as well as local buckling with bending, contradictorily past work mostly assumed that pipeline is under tension.

With day by day increasing capacity of computation and advancement in numerical modelling, one can find more facts for pipeline subjected to large motions including cases of pipe under compression as well. In this paper, past work is reviewed for pipeline subjected to large ground motion. A three dimensional FE based numerical model is suggested to carry out pipeline performance of buried pipeline subjected to large motion. A proposed model includes material nonlinearity, as well as it considers the large geometric deformation. For this purpose, three dimensional FE program is developed using MATLAB. Displacement controlled Arc-length technique is implemented to solve the nonlinear behavior. To reduce the computation time of analysis here parallelization tool kit of MATLAB is utilized.

* Corresponding author
E-mail address: ramancharla@iiit.ac.in (R. P. Kumar)

Keywords: Buried continuous pipeline; Large ground motion; Nonlinear-large deformation FEM; Displacement controlled Arc-length technique.

1. **Introduction**

Pipelines are common transportation means for oil and natural gas, which always act as an important lifeline facility for any nation. Generally, these pipelines are laid underground for economic, aesthetic, safety, and environmental reasons. While running through the length and breadth of a country the pipeline is exposed to diverse soil conditions. Presently, India operates and maintains 22,057 km (11,218 km of product, 8,528 km of crude oil, and 2312 km of LPG) of pipelines. Seismic hazard of pipeline is well demonstrated and documented during past several earthquakes all over the world. Predominant study for seismic hazard of pipeline started after the 1971 San Fernando earthquake. Newmark and Hall (1975) did the pioneer work for pipeline crossing the fault by assuming pipe as cable in their analytical study. The only force considered acting on the pipeline is the friction force at the pipe-soil interface along the longitudinal direction without lateral force offered by the soil. This model is further modified by Kennedy et al. (1977) by incorporating the lateral pressure offered by the soil. In 1985 Wang and Yeh further modified the model by dividing pipe into three regions depending upon the curvature in the pipeline. Region I is near the fault plane, while regions II and III are away from it. It was also assumed that strain in region II and III are elastic while the strain in region I is inelastic. For straight portion in region III they used the theory of beam on elastic foundation. In a model, they notify that maximum bending strain is in the region II and crucial combination of axial and bending strain will be at junction of II and III region, hence, concluded that the pipe would fail at this junction. It seems counter intuitive since one expects tensile ruptures at or very near to the fault crossing. Newly Karamitros et al. (2007) introduced a number of refinements in the method proposed by Wang and Yeh (1985). Previous method overlooked the effect of axial force on bending stiffness. Karamitros et al. suggested most unfavorable combination of axial and bending would not necessarily take place at the end of high curvature portion but within the zone, closer to the fault crossing point.

Likewise analytical models were developed for transverse PGD where pipeline was modeled with the assumption of small deformation. For the case of transverse PGD pipeline is mainly subjected to the bending. While in case of longitudinal PGD pipeline, it is exposed to the longitudinal tension and compression strains, which is less studied in the past.

In addition to the above-mentioned analytical models there are several numerical models proposed, which include a model for beam on nonlinear Winkler foundation. In which pipe is modeled with beam/shell elements and soil with springs (Takada et al. 1998). Nodes of the shell elements of the pipe are attached to soil that is modelled as springs. However,

these models are fine to pipeline but too harsh to the soil behavior, nevertheless the behavior of soil has significant impact on the pipeline response.

1.1 Scope

Though improved analytical models provide a good result, the models are developed with fundamental assumptions that the curvature of the pipeline on either side of fault plane is symmetrical. In case of strike slip fault the pipeline crossing essentially deforms in the horizontal plane where soil on either side of the pipeline extends to very large or for infinite distance. This offers the symmetric resistance to the pipe on either side in the plane of pipe deformation. This symmetry also takes care of point of contra- flexure to draw it closer to the pipeline fault crossing. Hence, the analytical models developed in the past are applicable to strike slip fault motions case only. For dip slip fault motion, the pipe-soil interaction forces along the fault motion are dissimilar due to great variation in the depth. Lesser depth of the soil above the pipe offers less resistance compared to bottom soil for deformed pipe. In addition to this, the deformation of the pipe greatly depends on the soil movement of the upper layer which usually differs in hanging wall and footwall. Hence, assumptions for identical curvature on either side of the fault plane is no longer valid. Analytical study is also restricted for pipeline under tension cases. Pipeline under compression usually involves the general as well as local geometric instability issues (e.g. pipeline during 1999, Izmit, Turkey earthquake (EERI, 1999)). Handling complex geometric stability is always hard to model in analytical studies. Faulting itself is phenomenon of large geometric changes, hence, theory of small deformation is no longer suitable for pipeline fault crossing which were used in the past. Hence, study of the pipeline under compression needs appropriate understanding as it involves both material as well as geometric failure.

However numerical models proposed by Takada et al. (1998), LIU Aiwen et al. (2004) for buried pipeline using shell element and nonlinear springs for pipe and soil, respectively, can perform for pipeline under compression. Though, post yielding of soil spring gives higher strain value in pipe. This could be the result of the inadequacy of the spring models to incorporate the actual soil behavior during soil yielding. In addition, these models do not consider the large geometric changes of upper soil layer, which has significant effect on pipeline performance. Stiffness of each individual spring is independent i.e. each spring behaves independently which disregard the effect of lateral soil confinement. Considering limitation of previous models and day-by-day increasing capacity, speed and powerfulness of the computer, the computer can make it possible to solve field problems by doing more realistic numerical analysis. Here, a more realistic numerical program using three dimensional FEM is developed for buried continuous pipelines. This program is developed using isoperimetric brick element.

The developed model takes care of material as well as large geometric changes to comprise fault motion.

2. Methodology

2.1 Numerical Modeling

The governing nonlinear finite element equation of solid continuum can be obtained from principle of virtual work. Eq.1 is adaptation from the one presented by K. J. Bathe (1996) and J.N. Reddy (2004) for updated Lagrangian approach.

$$\left({}_{t}^{t}K_{L}+{}_{t}^{t}K_{NL}\right)\Delta U^{(i)}={}^{t+\Delta t}R-{}_{t+\Delta t}^{t+\Delta t}F^{(i-1)} \tag{1}$$

Where,

$${}_{t}^{t}K_{L}=\int_{{}^{t}V}{}_{t}^{t}B_{L}^{T}\,{}_{t}D_{t}^{t}B_{L}\,d^{t}V$$

$${}_{t}^{t}K_{NL}=\int_{{}^{t}V}{}_{t}^{t}B_{NL}^{T}\,{}^{t}\tau\,{}_{t}^{t}B_{NL}\,d^{t}V$$

$${}_{t+\Delta t}^{t+\Delta t}F^{(i-1)}=\int_{{}^{t}V}{}_{t}^{t}B_{NL}^{T}\,{}^{t}\hat{\tau}\,{}_{t}^{t}B_{NL}\,d^{t}V$$

${}^{t}\hat{\tau}$ = Cauchy stress vector

B = Transformation matrix

${}^{t+\Delta t}R$ = vector of externally applied loads at time $t+\Delta t$

The numerical integration is performed according to Gaussian quadrature rule. A code is developed in MATLAB-7.9 for three dimensional FEA using 8 nodded isoparametric elements. The successes of any nonlinear analysis primarily depends on the accuracy, convergence, efficiency and stability of nonlinear solution technique. The nonlinear Eq. 1 can be solved by various nonlinear solution techniques available in the literature. Among this full or modified Newton-Raphson, method is simple to understand, implement and it generally converges in few iterations. However, this method fails to trace the nonlinear equilibrium path through the limit or bifurcation points, in vicinity of limit points, tangent stiffness matrix becomes singular and the iteration procedure diverges. This is common in buckling and strain softening nonlinear material behaviour type of the analysis. The displacement boundary condition in nonlinear analysis needs linearization of the prescribed boundary displacement, which can be easily incorporated in other methods like arc-length method. Hence, more robust arc-length method is employed for this work. Arc-length method was originally developed by Riks (1972; 1979) and Wempner (1971) and later modified by several researchers.

2.2 Arc-length Method

Though this method was developed in 70s a number of modifications have been suggested in the past few years. One can find elementary of the method from any standard literature either from Riks (1972, 1976) papers or Crisfield (1981) etc. Generally there are two approaches which are used, a fixed arc length and varying arc length. The fixed arc length is suitable for load and/or forced controlled, while for path following method, new arc-length is evaluated at the beginning of each load step to ensure the achievement of the solution procedure. The success of the path following method depends on three essential stages. Firstly, proper selection of root for quadratic equation obtained by simplifications of the additional constrains equation, which leads to a quadratic equation in terms of the incremental load factor. Secondly, is predicting the value of the load-factor for each increment. Generally, load-factor for current increment is computed depending on the rate of convergence of the solution process in previous increment. For first increment, trial value is assumed as 1/5 or 1/10 of total load (Memon et al. 2004). Finally, to avoid the doubling back of the equilibrium path, determination of the sign for the predicted load factor needs sufficient alertness. In case of divergence from the solution path, the arc-length is reduced and computations are done again.

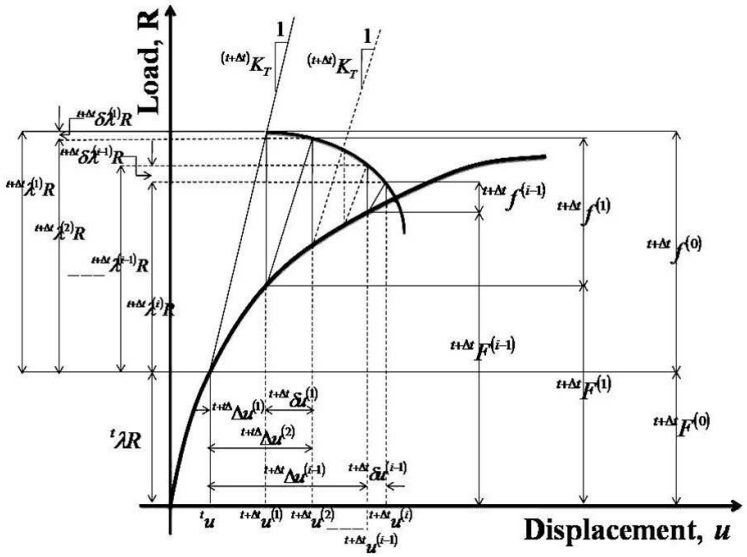

Figure 1. Iterative Procedure for Arc-Length Method

Generally, incremental equations in structural nonlinear static analysis take the following form:

$$^{t+\Delta t}f^{(i-1)} = {}^{t+\Delta t}F^{(i-1)} - {}^{(t+\Delta t)}\lambda^{(i-1)}R \qquad (2)$$

Where, $^{t+\Delta t}f$ = the out of balance force, λ = a scalar, known as load level parameter, which is considered as an unknown parameter and *R* is a given fixed external force vector. The

incremental displacement for current load step with modified Newton-Raphson method assumption of fixed K_T is calculated as,

$$ {}^{t+\Delta t}\delta u^{(i-1)} = {}^{t+\Delta t}\delta \bar{u}^{(i-1)} + \delta^{(t+\Delta t)}\lambda^{(i-1)} \cdot \delta^{t+\Delta t}\hat{u} \tag{3} $$

Where

$$ {}^{t+\Delta t}\delta \bar{u}^{(i-1)} = -\left(K_T^{-1}\right) {}^{t+\Delta t} f^{(i-1)} \tag{4} $$

and

$$ \delta^{t+\Delta t}\hat{u} = -\left(K_T^{-1}\right) \cdot R \tag{5} $$

Note that the K_T is evaluated at the end of using the converged solution ${}^{(t)}u$ of the last load step (Fig. 1). Hence improved prediction of the equilibrium configuration can be obtain as

$$ {}^{t+\Delta t}u = {}^{t}u + {}^{t+\Delta t}\Delta u^{(i)} \tag{6} $$

$$ {}^{t+\Delta t}\Delta u^{(i)} = {}^{t+\Delta t}\Delta u^{(i-1)} + {}^{t+\Delta t}\delta u^{(i-1)} \tag{7} $$

$$ {}^{t+\Delta t}\lambda^{(i)} = {}^{t+\Delta t}\lambda^{(i-1)} + \delta^{t+\Delta t}\lambda^{(i-1)} \tag{8} $$

For the first iteration of the first load step it is assumed that u = 0, for the first iteration of other than first load step $\delta^{t\neq 1}\lambda^{(1)}$ can be calculated from incremental arc-length form written as,

$$ \Delta u \cdot \Delta u + \lambda^2 \psi^2 R \cdot R = \Delta l^2 \tag{9} $$

Where Δu and λ are converged incremental quantities, Δl is fixed radius of desired intersection, and ψ is the scaling parameter for loading terms, for cylindrical arc-length method, ψ = 0 (Crisfield, 1981); while for the spherical arc-length methods ψ = 1. For cylindrical arc-length Eq. 9 simplified as,

$$ {}^{t+\Delta t}\Delta u^{(i)} \cdot {}^{t+\Delta t}\Delta u^{(i)} = \Delta l^2 \tag{10} $$

Substituting for ${}^{t+\Delta t}\Delta u^{(i)}$ from Eq. 7 gives quadratic equation for incremental in the load parameter ${}^{t+\Delta t}\delta u^{(i-1)}$,

$$ A_1\left[{}^{t+\Delta t}\delta u^{(i-1)}\right]^2 + A_2\left[{}^{t+\Delta t}\delta u^{(i-1)}\right] + A_3 = 0 \tag{11} $$

Where,

$$ A_1 = \delta^{t+\Delta t}\hat{u} \cdot \delta^{t+\Delta t}\hat{u} $$

$$ A_2 = 2\left({}^{t+\Delta t}\Delta u^{(i-1)} + {}^{t+\Delta t}\delta \bar{u}^{(i-1)}\right)\delta^{t+\Delta t}\hat{u} $$

$$ A_3 = \left({}^{t+\Delta t}\Delta u^{(i-1)} + {}^{t+\Delta t}\delta \bar{u}^{(i-1)}\right) \cdot \left({}^{t+\Delta t}\Delta u^{(i-1)} + {}^{t+\Delta t}\delta \bar{u}^{(i-1)}\right) - \left(\Delta l\right)^2 $$

To avoid the tracking backing the equilibrium path Crisfield suggested that the root should be such that the angle between the incremental solutions at two consecutive iterations $\Delta u^{(i-1)}$ and $\Delta u^{(i)}$ be minimum. The incremental load factor λ is updated according to Eq. 8.

2.2.1 The Predictor Solution

The auto-selection and auto-adjustment of the arc-length increment in each incremental step are very important, which are related to the correctness and efficiency of the numerical algorithms. In order to do that, the convergent information in the last arc-length incremental step is very useful and must be analyzed. The main equation in controlling the arc-length increments available is as follows:

$$^{t+\Delta t}\Delta l = {}^{t}\Delta l \cdot \left(\frac{I_d}{I_0} \right)^n \tag{12}$$

Where, $^{t}\Delta l$ is the arc-length used in the last iteration of last increment, I_d is the number of desired iterations (usually < 5) and I_0 is the number of iterations required for convergence in the previous step. Crisfield suggested that n should be set to ½. The first arc-length is computed as

$$\Delta l = \delta^1\lambda^{(1)} \sqrt{\delta^1\hat{u} \cdot \delta^1\hat{u}} \tag{13}$$

Hence, the incremental load factor for cylindrical arc-length method can be predicted as

$$\delta^1\lambda^{(1)} = (\pm)\frac{\Delta l}{\sqrt{\delta^1\hat{u} \cdot \delta^1\hat{u}}} \tag{14}$$

The choice of the sign of the incremental load factor in the predictor phase of arc-length methods is known to be of paramount importance in determining the success of such procedures in tracing unstable equilibrium paths. If the wrong sign is predicted, the solution sequence `doubles back' on the original load-deflection curve and the arc-length method fails to trace the complete path. Many procedures have been proposed to predict the continuation direction, i.e., to choose the sign of $\delta\lambda$ in the predictor solution such that it does not `track back' on the current path. The most popular ones appear to be the predictors based on

(a) *The sign of current tangent stiffness determinant*. Follow the sign of $|K_T|$

$$\text{sign}(\delta\lambda) = \text{sign}(|K_T|)$$

(b*) Incremental work*. Follow the sign of the predictor work increment:

$$\text{sign}(\delta\lambda) = \text{sign}\ (\delta\hat{u}^T R)$$

(c*) The predictor criterion of Feng* follow the sign of history of the current equilibrium path and the current tangential solution.

$$\text{sign}(\delta\lambda) = \text{sign}\ (\delta\hat{u}^T \Delta u)$$

Procedure (a) is widely used and works well in the absence of bifurcations. In the presence of bifurcations, however, it is known not to be appropriate and fails in most cases. As pointed out by Crisfield, its ill behaviour stems from the fact that the sign of $|K_T|$ changes either when a limit point or when a bifurcation point is passed. In this case, the predictor cannot distinguish between these two quite different situations, unless further analyses are undertaken. In the presence of a bifurcation, instead of following the current path, the solution will oscillate about the bifurcation point. E.A. de Souza (1999) stated that the procedure (b), on the other hand, is `blind' to bifurcations and can continue to trace an equilibrium path after passing a bifurcation point. However, this criterion proves ineffective in the descending branch of the load-deflection curve in `snap-back' problems, where the predicted positive `slope' will provoke a `back tracking' load increase. Feng et al. (1996) proposed a direction prediction criterion (c), whereby, the sign of the predictor load factor is made to coincide with the sign of the internal product between the previous converged incremental displacement Δu and the current tangential solution, $\delta\hat{u}^T$. A key point concerning the above criterion is the fact that Δu carries with it information about the history of the current equilibrium path. E.A. de Souza (1999) showed by means of geometric arguments that the resulting predictor of Feng et al. (1996) approach can easily overcome the problems associated with criteria (a) and (b).

2.3 Validation of Code

For the validation of developed code, tests have been performed on the 3D cantilever beam. Load- deflection curve is compared with commercially available finite element package ANSYS-12. Material behavior assumed for the test is same as pipe material. Beam dimensions, meshing and point load considered at free end are given in Table 1. Figure 2 shows perfectly matching load-deflection curve obtained from developed code and ANSYS.

2.4 Model Dimensions

The coordinate system and notations used for this work are shown in Figure 3. In reality, soil media does not have any fixed boundaries or can be assumed at infinite distance, which is virtually impossible to incorporate in the numerical model, hence model dimensions are determined for boundary effect and it is considered as 80m (L) x 12m (H) x 15m (W).

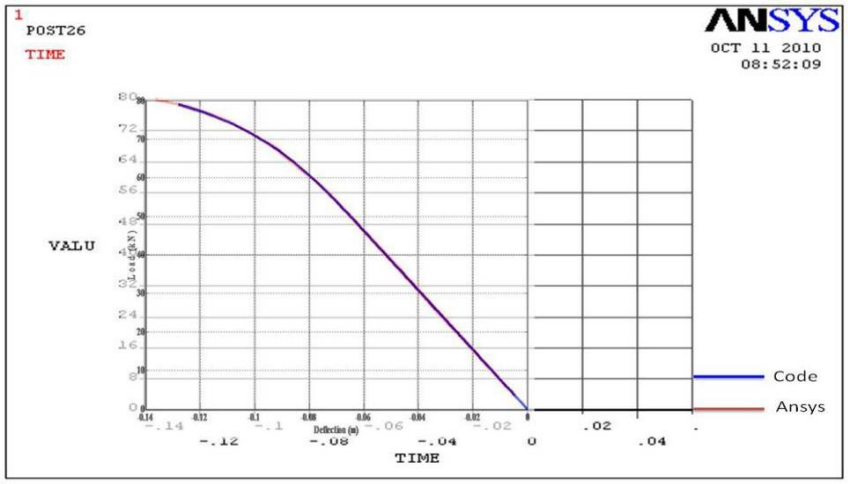

Figure 2. Comparison of results between ANSYS and FE code.

Table 1. Comparison of Code and ANSYS results

L x D x B (m)	Element size (m)	Point load (kN)	U_{max}(m)	
			Model	ANSYS
3.0 x 0.2 x 0.05	0.05 x 0.05 x 0.05	80	0.130	0.135

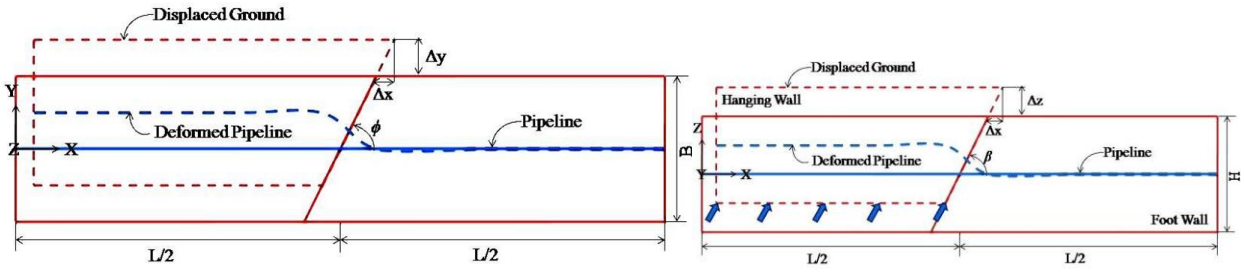

(a) (b)

Figure 3 (a). Plan view of buried pipeline model for strike-slip fault motion. (b)Sectional view of buried pipeline model for dip-slip fault motion.

The pipe near the fault usually suffers large deformation, which is not so long, about 10m to 30m, and the damaged point of pipe also occurs in this pipe segment (LIU Ai-wen, 2004). For this, meshing of varying element lengths is considered to optimize the memory and time usage. Finer meshing of 0.5 m element lengths are used near the fault region for 20m distance on either side. Then for remaining length 1m, element size is used. Pipe is divided

in eight equal divisions in circumferential direction and single division is made for wall thickness. Near the pipe, soil is meshed by small elements with varying size for the square region of 1.2m (Fig. 4). Elements size of soil, which is far from the pipe, is taken as 1.5m.

Default parameter in evaluation of pipeline performance are considered as maximum fault offset (Δ_{max}) = 0.6m, pipeline fault crossing angle (ϕ) = 90^0, diameter of the pipeline (D) = 0.61m (24inches), pipeline wall thickness (t_p) = 0.0095m (0.375 inches) and depth of the buried pipelines(d_b) = 0.91m (3feet). Performance is evaluated for no internal pressure condition. Few assumptions are made in the development of the models. It assumed that perfect bond exists between the soil and pipe material.

2.5 Boundary Conditions

The target ground displacement in all the models are applied at the bottom, with the free top boundary conditions. While on the side boundaries, all nodal degree of freedoms other than in the direction of the components of targeted displacements are constrained. In case of fault model, total soil mass block is divided into two parts, on either side of the fault plane. The fault displacement (Δ) is applied to only one soil block by keeping other one fixed.

In case of the transverse PGD model, lateral displacement is idealized by using beta probability density function suggested by T. O'Rourke and summarised as,

$$y(x) = \delta \left[\frac{s}{s_m}\right]^{r'-1} \left[\frac{1-s}{1-s_m}\right]^{\tau-r'-1} \quad 0 < s < 1 \qquad (15)$$

Where s_m = 0.5, r' = 2.5 and τ = 5.0. The maximum PGD (δ) here in this study is taken as 2m with the width of PGD zone W = 10, 30 and 50m.

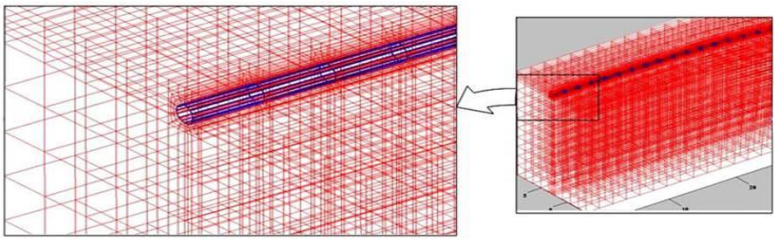

Figure 4. Proposed finite element model of buried pipeline.

2.6 Material Modeling

For pipe Ramberg-Osgood relationship is one of the most widely used models (M. O' Rourke 1999, IITK-GSDMA GUIDELINES 2007), while for soil hyperbolic model is common (S.L Kramer (2007)). Hence, the same are used in these studies which are summarized below:

$$\varepsilon = \frac{\sigma}{E}\left[1 + \frac{n}{1+r}\left(\frac{\sigma}{\sigma_y}\right)^r\right] \qquad (16)$$

Where,

ε = Engineering strain

σ = Stress in the pipe

E_i = Initial Young's modulus

σ_y = Yield strain of the pipe material

r, n = Ramberg - Osgood parameters adopted as r = 31.50 and n= 38.32 Karamitros (2007)

While the hyperbolic soil model is given as,

$$\tau = \frac{G_{max}\,\gamma}{1+\left(G_{max}/\tau_{max}\right)|\gamma|} \qquad (17)$$

where

τ = shear stress,

γ = shear strain

G_{max} = maximum shear modulus

τ_{max} = maximum shear stress

The API5L-X 65 steel pipe is frequently used in literature (Newmark and Hall, 1975, Karamitros 2007 etc.), hence, the same is adopted for this study. Table 2 shows the properties used for API5L-X 65 pipe material. While soil is assumed as typical sand with initial Young's modulus as Ei = 50Mpa and Poisson ratio 0.4. Table 3 shows constants used in hyperbolic model.

Table 2: Properties of AP15L-X 65 Pipe

Properties for API5L X-65 Pipe	**Magnitude**
Initial Young's Modulus (E_i)	210 Gpa
Yield Stress (σ_y)	490 Mpa
Failure Stress (σ_f)	513 Mpa
Failure Strain (ε_f)	4%
Poisson's ratio (μ)	0.3
Density (ρ_p)	7.8g/cm^3

Table 3. Constants for Hyperbolic Model

Medium density sand properties	**Magnitude**
Maximum Shear Modulus (G_{max})	60 Mpa
Maximum shear Strength (τ_{max})	0.0216 Map
Failure Stress (σ_f)	513 Mpa
Density (ρ_s)	1.44/cm^3

3. Results and Discussion

The performance of continuous buried pipeline crossing active fault is studied using proposed finite element models. The developed model can be implemented for all sorts of fault motion with variation in other geometric parameters. Here case of strike slip is taken to determine the influencing on the performance of pipeline for the fault offset (Δ), pipeline-fault crossing angle (β), wall thickness to diameter ratio ($\frac{t_p}{D}$) depth of the buried pipeline (d_b) and their combinations. In the nonlinear numerical analysis of soil the maximum ground displacement is generally restricted up to 5% of the total depth of the model beyond which results usually deviate and are unrealistic, hence, maximum component of fault offset is limited to 0.6m. Total fault offset of 0.6m is applied with an increment of 0.1m. Pipeline fault plane angle is varied from 40^0 to 140^0 with an increment of 10^0. The pipeline wall-thickness 0.0095, 0.0103 and 0.0190 are considered, while depth is varied from 2 to 4 feet.

3.1 Pipeline subjected to Strike Slip Fault Motion

3.1.1 Effect of the Fault Offset

Hence for ϕ = 90^0 the pipeline is mainly subjected to bending; while for positive ϕ the small angle pipeline will be under pure compression. Hence, for determining the effect of the fault offset a 60^0 angle is chosen, where effect of both the direct and bending strain can be seen. Figure 5 shows the effect of the fault offset on total and bending strain distribution in the pipeline. Maximum fault offset 0.6m is applied with an increment of 0.1m. Generally two kinds of failure are associated with pipeline, first material failure when pipe material is strained beyond sustainable limit and in general yielding strain and geometric failure in which geometry of the pipe is so distorted that pipeline becomes inadequate to pass the fluid. From figure 5 (a) it can be seen that maximum strain (ε_{xx} = 0.00186) generating in the pipeline for fault offset 0.2m is just below the yield strain (ε_y = 0.002). From which it

can be said that the pipe does not have any serious damage up to 0.2m fault offset. Thereafter the difference of the strain curve, near the fault plane continuously increases. This indicates that pipe material enters plastic stage. While discussing about the pipeline damage there are two points, which are most significant. First, how much material has yielded and secondly how much length of the pipe enters in the plastic stage. This has great significance in case of post event repair and maintenance. This large longitudinal strain in the pipe material further causes reduction in the wall thickness (developing upon Poisson ratio), which may not be safe design thickness for the internal pressure and other load.

From figure 5(a) one can see that for the 0.3m fault offset only near the fault plane about10m pipe length is beyond the yield strain. While majority of the pipe length just crosses the yield strain. Thereafter both length of pipeline crossing yield point and maximum strain beyond the yield strain is increasing seriously. For the considered cases no large geometric failure is observed. From bending strain distribution curves (Fig. 5b) one can observe that bending strain in the pipe is smoothly increasing up to the 0.4 fault offset. After that the bending strain distribution curve is slightly disturbing for 0.5 and 0.6m fault offset at 10m on either side of the fault plane. This kind of disorder mainly signifies the local buckling on the pipe.

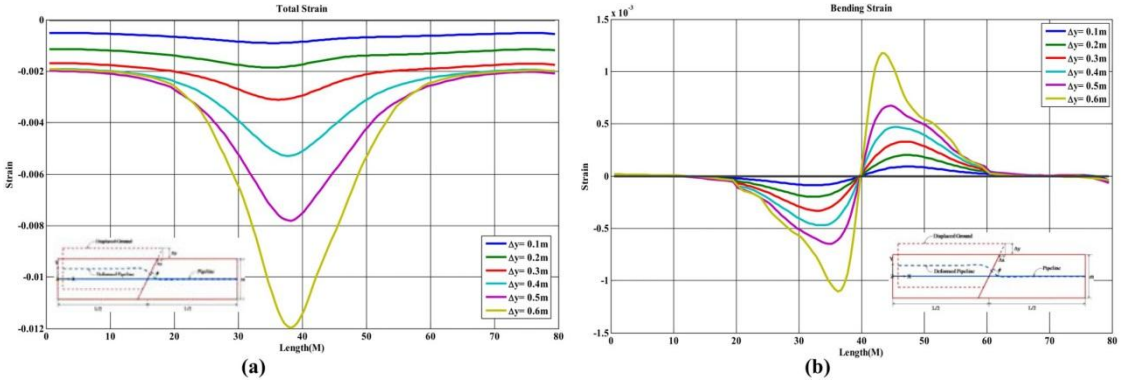

Figure 5. Effect of fault offset on strain distribution for strike slip with *Δy* = 0.1m to 0.6 m and*ϕ=60⁰*(a) Total strain effect. (b) Bending strain effect.

3.1.2 Effect of the Pipeline Fault Angle

The pipeline fault angle is second most vital parameter related to the pipeline performance. Hence effect of the pipeline-fault angle (ϕ) is studied by varying the pipeline-fault angle from 40^0, 60^0, 80^0, 90^0, 100^0, 120^0to140^0 for fault offset of 0.6m. The performance analysis of pipeline becomes more complex due to unlike behavior of the pipeline under compression and tension. In general, under tension the pipe fails due to excessive straining of pipe material, while in case of compression in addition to the material failure geometric

failure also takes place. The foremost point that can be observed in the strain distribution curve plotted in figure 6 is that the maximum strain developing for negative pipeline fault angle ($\phi < 90^0$) is much higher than the positive pipeline fault crossing angle ($\phi > 90^0$). The reason for this can be understood as, when pipeline is subjected to the compression the pipe has a chance of bending and/or buckling and hence the fault offset is accommodated by the geometric change without much internal deformation, which leads to lesser internal deformation in the pipe. There are two fundament troubles associated with the pipeline buckling, firstly it is a sudden phenomenon and may adversely affect the operational pipelines.

Secondly, the large geometric distortion during buckling further causes pressure loss in the pipeline, which is the foremost significant parameter for the petroleum pipeline. In case of pipeline under tension the whole fault displacement at the pipe fault crossing is needed to accommodate the internal deformation of pipeline material.

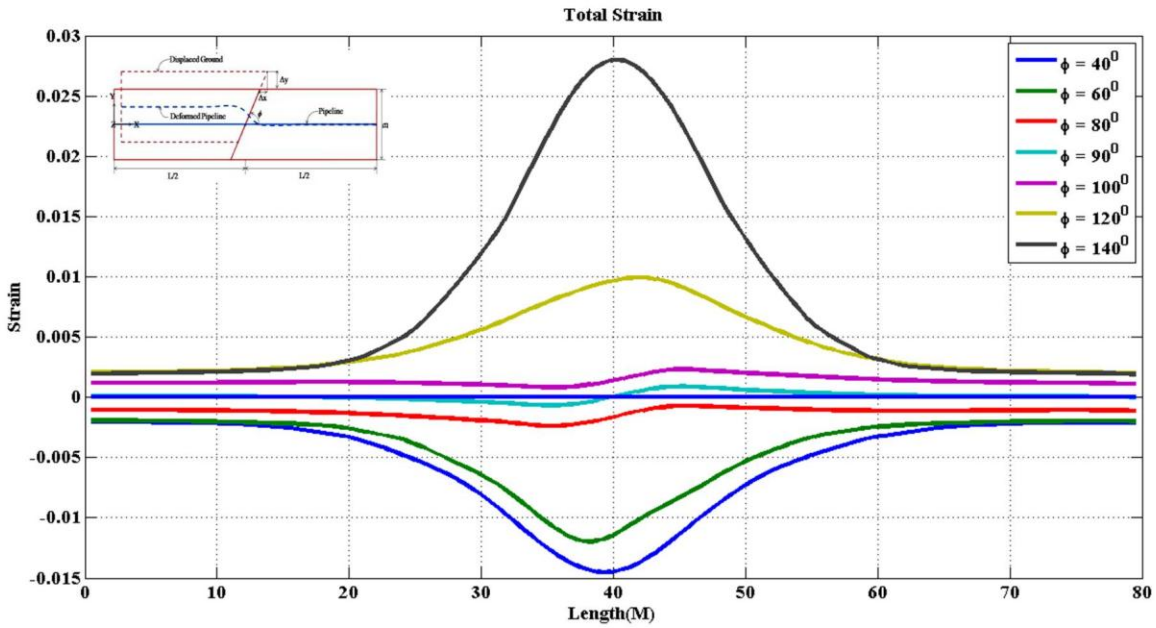

Figure 6. Effect of pipeline fault angle on total normal strain distribution for strike slip with Δy =0.6m

From figure-6 it can also be observed that for $\pm 80^0$angle the total normal strain distribution is similar on the opposite sides of zero strain axes. This indicates that the buckling of the pipe does not take place for all pipeline fault angles.

3.1.3 Effect of Pipeline Wall Thickness to Diameter Ratio

In general, design of the wall thickness is the main function of internal pressure. Where it is designed for hoop and longitudinal stresses and checked for secondary loads like overburden and live loads. Nevertheless, the present study shows that the thickness to diameter ratio has great hold on the pipeline performance crossing strike slip fault especially when pipeline is subjected to the compression. To understand the effect of the wall thickness here 0.0095, 0.0136 and 0.0190 are the three wall-thicknesses to diameter ratios considered. To have an effect of geometric failure under compression the parametric study is performed for ϕ = 40^0 where pipe can be subjected to sufficient compression.The maximum fault offset applied here is 0.47m after which the pipe is subjected to large geometric changes which further causes soil failure and diverges numerical analysis.

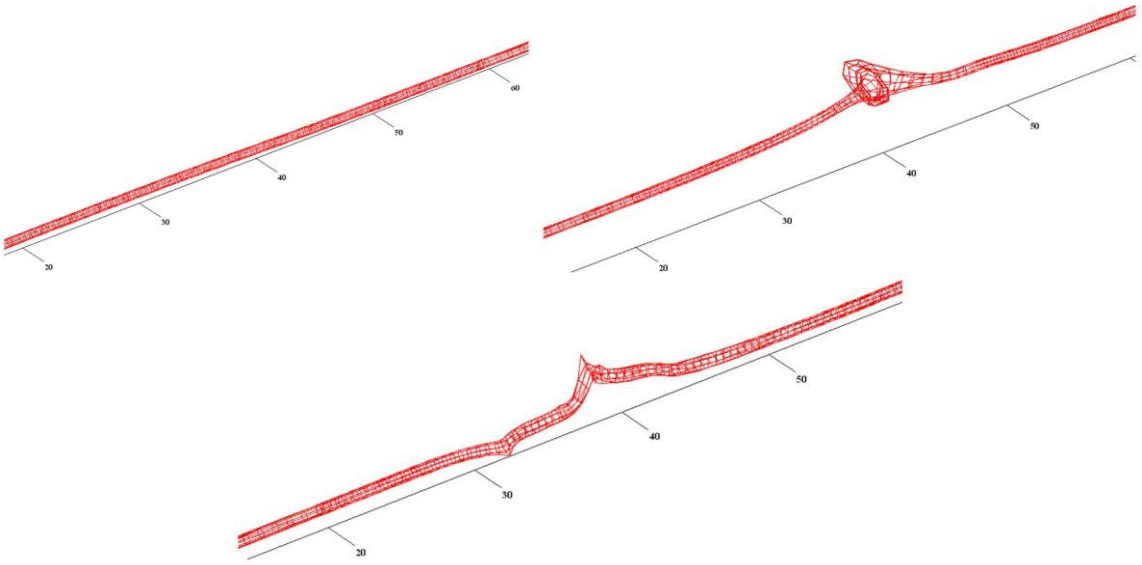

Figure 7. Effect of pipeline wall thickness to diameter ratio for strike slip with Δy = 0.46m and ϕ = 40^0

Geometric failure of the pipe can be more clearly understood by observing the deformation of the pipe. Hence, for deformed shapes of the pipes with different wall thickness to diameter ratios are plotted in figure 7. From figure, it can be clearly seen that pipe with thicker wall thickness is subjected to more geometric changes than the pipe with thinner wall thickness. However, thicker wall pipe has higher internal deformation capacity, which can be observed in the strain distribution figure 8. Nevertheless for a less strain, the thicker pipe got more damage. This clearly indicates geometric failure of the thick wall pipe. The reason for this is quite understandable as the thinner wall pipe has lesser moment of inertia and can easily bed and deform to accommodate the fault displacement. On other hand the thicker wall pipe, which is subjected to less strain indicates lesser internal

deformation, therefore thick wall pipe needs to accommodate fault displacement by large geometric deformations. From the above discussion, it is clear that when pipe is subjected strike-slip fault with $\phi < 90^0$, thicker pipes are more vulnerable to geometric failure.

If we observe the deformed shape of the pipe in figure 7, it can be seen that the pipe with 0.0095 wall thickness to diameter ratio is deformed only in the horizontal plane which indicates bending of the pipe with strike-slip fault motion. While in case of $(\frac{t_w}{D}) = 0.0136$ the pipe looks like little moved with fault and then bulged in horizontal plane indicating geometric failure in plastic stage. Finally in case $(\frac{t_w}{D}) = 0.0190$ the pipe is purely buckled in vertical plane, which is catastrophic geometric failure. At much lesser depth the depth of top soil compares to three remaining directions offering lesser resistance to the buckling of pipe. That could be the reason why a strong pipe is buckled in vertical plane.

3.1.4 Effect of the Buried Depth

Here, the effect of the buried depth of pipeline is determined for 2feet, 3feet and 4feet depth. The fault offset applied here is 0.6m with pipeline fault angle 60^0. From Figure 9 it is clearly seen that there is no significant effect of the depth on the strain distribution. Fault displacement and pipe deformations are happening in the horizontal plane while effect of depth is more significant in vertical plane. In addition, the assumption made in the model for perfect bonding between pipe and soil diminishes. In case of frictional forces the overburden pressure plays a vital role, which directly depends on the buried depth of the pipe.

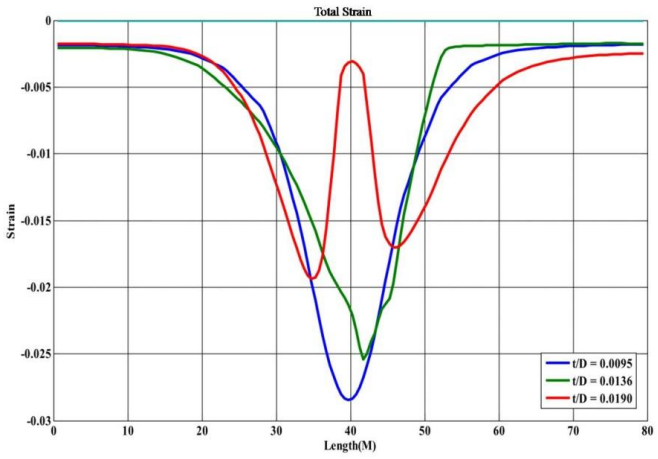

Figure 8. Effect of pipeline wall thickness to diameter ratio for strike slip with Δy = 0.46m and $\phi = 40^0$

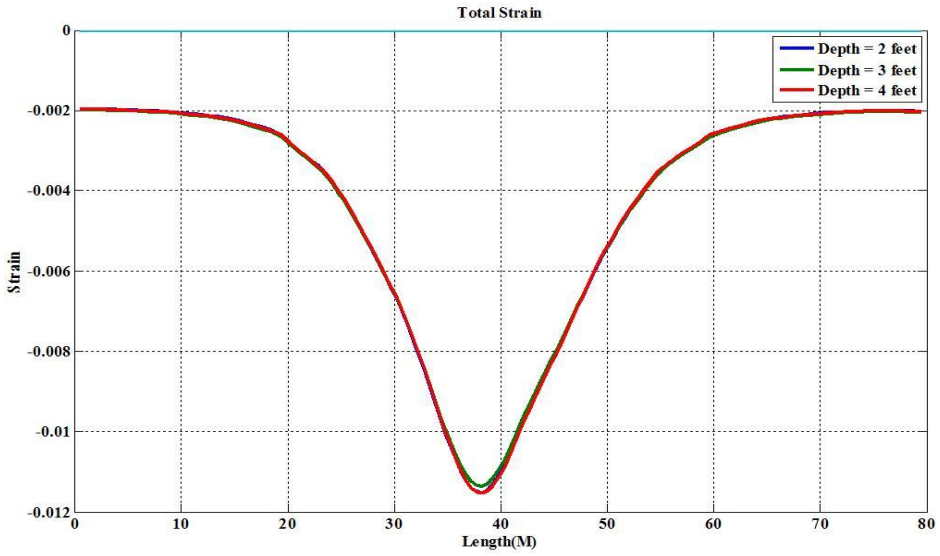

Figure 9. Effect of buried depth for strike slip with Δy = 0.6m and $\phi = 60^0$

3.2 Pipeline Subjected to Transverse PGD Motion

3.2.1 Effect of PGD Zone Width

The effect of zone width is plotted in figure 10. The maximum displacement applied here is 0.6m with zone width varying from 10m to 60m. The maximum strain (-8×10^{-4}) developed here for the considered cases is less than the yield strain (20×10^{-4}) indicating that for the considered case the pipeline is safe and does not yield. From the figure it can be said that the zone width has great influence on the strain distribution in the pipe. The total effect of zone width can be considered in terms of maximum strain developing in the pipe, width of compression zone and local buckling effect. The maximum strain developing in the pipeline on both tension and compression sides are significantly changing with zone width when offset of 0.6m is applied. From the results, it can be observed that the strain in the pipe is increasing with the zone width up to 30m, thereafter the strain of the pipe is further reducing for the larger zone width. This phenomenon can be understood in terms of the upper soil movement and pipe length participating for the PGD. For the initial stage up to 30m zone width, relatively shorter zone width of soil need more deformation to accommodate base ground movement. This offers higher resistance to ground movement and leads to lesser displacement of the upper soil layer, hence, the pipe displaces for smaller deformation, which further leads to lesser strain in the pipe. Thus, it can be abridged as small PGD zone width more soil deformation (i.e. higher resistance) and lesser upper soil layer movement lead reduced strain in the pipe. On the other hand, as the zone width increases, more soil can take part in the PGD, which can deform easily and can displace more, leading to more strains in the pipe. However, this phenomenon takes place

only up to restricted PGD zone width (e.g. in this case up to 30m), thereafter the maximum upper soil displacement is stabilized for given base ground movement.

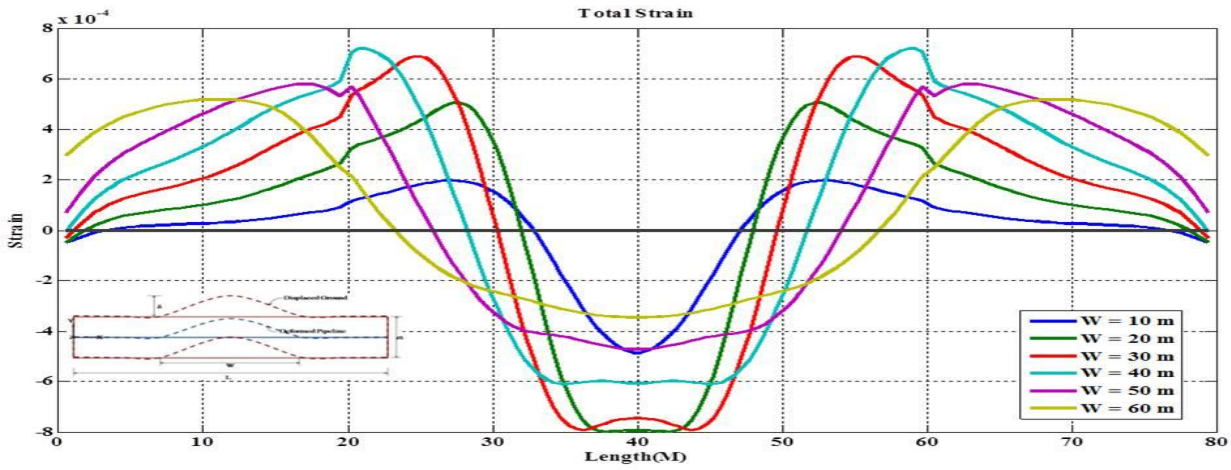

Figure 10. Effect of zone width on strain for transverse PGD with δ = 0.6m and W = 10 m to 60m

However, with the increment in the PGD zone more pipe length is available for accommodating the ground displacement. As the strain is distributed over a large length that further shifts the point of contra-flexure apart and increases the compression zone width of the pipe.

Another significant point here that can be seen is the local buckling effect.For sure, the local buckling of the pipe is a vast subject and cannot be covered in this work. However, few observations here can be made from figure 10. For the case of 20 and 30m zone width, maximum strain level in the pipe is more or less same, though one can see that pipe subjected to 30m zone width is exposed to higher buckling. The reason could be the pipeline length under compression is increasing with the PGD zone width that makes pipeline to easily buckle. Strain drop for the buckling cases are more for example for the case of 10m and 50m zone width, maximum compressive strain levels are same but pipeline subjected to 50m zone width has higher positive strains.

4. Conclusions

Main conclusions of this study can be stated as the following:

- Numerical modeling of physical problem if implemented with latest updated methods could yield much better results.
- Apart from material behavior and its failure, geometrical behavior becomes important when studies are done on pipes subjected to large ground motions.

- Compression failure behavior of the pipelines is catastrophic in nature as it leads to sudden buckling. Which crucially depends on the pipe wall thickness.
- A strike-slip numerical study of buried pipelines with different parameters has shown the effect of both direct and bending strain.
- Though here developed model is implemented on the strike slip fault motion but the same can be implemented for other kinds of ground motions.

References

Bathe, K. J (2002). Finite Element Procedures, *Prentice-Hall of India Private Limited, New Delhi.*

Dimitrios K. K., D. B. George, and P. K. George (2007). Stress analysis of buried steel pipelines at strike-slip fault crossings, *Soil Dynamics and Earthquake Engineering*, 27(3), 200–211.

Neto, E.A. de Souza, and Y.T. Feng (1999). On the determination of the path direction for arc-length methods in the presence of bifurcations and snap-backs , *Computer Methods in Applied Mechanics and Engineering*, 179, 81–89.

EERI (1999). The Izmit (Kocaeli) Turkey, Earthquake of August 17, 1999, *EERI Special Earthquake Report.*

Feng, Y. T., D. Peric, and D. R. J. Owen (1996). A new criterion for determination of initial loading parameter in arc-length methods, *Computers and Structures*, 58 (3), 479–485.

IITK-GSDMA (2007). Guidelines for seismic design of buried pipelines.

Reddy, J. N. (2004). Introduction to nonlinear finite element analysis, *Oxford University Press.*

Kennedy, R. P., R. A. Williamson, and A. M. Chow (1997). Fault Movement Effects on Buried Oil Pipeline, *Transportation Engineering Journal*, 103(5), 617–633.

Liu, A. W.., Y. X. Hu, F. X. Zhao, X. J. Li, S. Takada, and L. Zhao (2004). An equivalent-boundary method for the shell analysis of buried pipelines under fault movement, *Acta Seismologica Sinica*, 17(1), 150–156.

Memon, B. A., and X. Z. Su(2004). Arc-length technique for nonlinear finite element analysis, *Journal of Zhejiang University Science*, 5(5), 618–628.

Newmark N. M., and W. J. Hall (1975). Pipeline design to resist large fault displacements, *U.S. National Conference on Earthquake Engineering*, 416–425.

Riks, E. (1972). The application of Newton's method to the problem of elastic stability, *Journal of Applied Mechanics*, 39(4), 1060–1065.

Riks, E., (1979). An incremental approach to the solution of snapping and buckling problems, *International Journal of Solids and Structures*, 15(7), 529–551.

Rourke, M. J., and X. Liu (1999). Response of buried pipelines subject to Earthquake Effects, *Multidisciplinary centre for Earthquake Engineering and Research, Monograph No*.3.

Rourke M. J. (1988). Critical aspects of soil-pipe interaction for large ground deformation, *Proc., 1st Japan-US Workshop on Liquefaction, Large Ground Deformation and their effects on Lifeline Facilities*, 118-126

Takada, S, J. Liang, and T. Li (1998). Shell-Mode Response of Buried Pipelines to Large Fault Movements, *Journal of Structural Engineering*, 44A, 1637–1646.

Wang, L. R. L., and Y. H. Yeh (1985). A Refined Seismic analysis and Design of Buried Pipeline for Fault Movement, *Earthquake Engineering and Structural Dynamics*, 13(1), 75–96.

Wempner, G.A, (1971). Discrete approximation related to nonlinear theories of solids, *International Journal of Solids and Structures*, 7(11), 1581–1599.

Ministry of Petroleum and Natural Gas Government of India, New Delhi (Economic Division) (2011-12). Basic Statistics on Indian Petroleum & Natural Gas